ACS OMEGA

http://pubs.acs.org/journal/acsodf

Article

Controlling Miscibility of the Interphase in Polymer-Grafted Nanocellulose/Cellulose Triacetate Nanocomposites

Hiroto Soeta, Shuji Fujisawa, Tsuguyuki Saito, and Akira Isogai*

Cite This: *ACS Omega* 2020, 5, 23755−23761

Read Online

ACCESS | Metrics & More | Article Recommendations | Supporting Information

ABSTRACT: The miscibility at the interphase of polymer-grafted nanocellulose/cellulose triacetate (CTA) composite films was tailored using different casting solvents. The polymer-grafted cellulose nanofibrils were prepared by modifying surfaces of 2,2,6,6-tetramethylpiperidine-1-oxyl-oxidized nanocellulose with amine-terminated poly(ethylene glycol) (PEG). The PEG-grafted nanocelluloses were individually dispersed in dichloromethane, 1,4-dioxane, and *N*,*N*-dimethylacetamide. The PEG-grafted nanocellulose/CTA composite films were prepared by mixing the nanocellulose dispersion and CTA solution and subsequent casting-drying. The miscibility of PEG and CTA at the interphase of the composite was controlled by controlling the solvent, which was confirmed by dynamic mechanical analysis. All the composite films showed high optical transparency. However, the mechanical properties of the composites differed because of the difference in the PEG/CTA interfacial miscibility. The composite films with better PEG/CTA interfacial miscibility showed higher Young's modulus, strength, and toughness. This interfacial design technique paves the way to exploiting the reinforcing potential of highly transparent and hydrophobic surface-grafted nanocellulose/polymer composite materials.

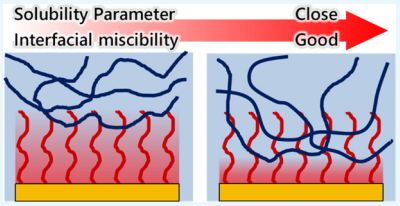

INTRODUCTION

Nanosized reinforcements such as nanocellulose, carbon nanotubes, and clay have been shown to provide superior reinforcement to conventional materials because of their high mechanical stiffness, high aspect ratio, and large surface area.[1,2] Numerous studies have incorporated nanofillers into polymer matrices to improve the mechanical and thermal properties.[3−6]

Reinforcing can be maximized by improving the dispersibility of the nanofiller and compatibility between the nanofiller and polymer matrix. Many approaches for improving these properties have been explored.[7−11] A common approach is surface modification of the nanofiller, such as by introducing functional groups to improve the surface wettability toward the matrix polymers.[12,13] Polymer grafting has also been used to enhance the interfacial compatibility between nanofillers and matrices.[14−17] It has been reported that grafting an identical polymer with the matrix can significantly improve the interfacial compatibility and stress−transfer efficiency between the nanofiller and polymer matrix.[17,18] However, these surface modifications are likely to change the dispersibility of the nanofiller in the matrix, which may deteriorate the reinforcing effect. The dispersibility of the nanofiller is also affected by the solvent used to prepare the composite.[19−22] Therefore, it is difficult to improve the interfacial compatibility without changing the dispersibility of the nanofiller, although both good interfacial compatibility and good dispersibility are required to exploit the reinforcing effect of the nanofiller. Few studies have systematically investigated the contribution of interfacial compatibility to the reinforcing effect of individually dispersed nanofillers on the properties of composites.

We previously reported the contributions of interfacial thickness and grafting density of 2,2,6,6-tetramethylpiperidine-1-oxyl (TEMPO)-oxidized cellulose nanofibers (TOCNs) to the composite properties.[23,24] The surfaces of the TOCNs were modified with amine-terminated polyethylene glycol ($PEG\text{-}NH_2$). The TOCNs were individually dispersed in the cellulose triacetate (CTA) matrix with and without surface modification when they were prepared from *N*,*N*-dimethylacetamide (DMAc) dispersion.[24] The interfacial structures were thus tailored by controlling the molecular weight and grafting ratio of $PEG\text{-}NH_2$ without changing the dispersibility of the TOCNs in the polymer matrices. We also prepared the PEG-grafted TOCN (PEG-TOCN)/CTA composite films as an optically transparent film from dichloromethane (DCM) dispersion.[25] In this study, the mechanical properties of the CTA matrix were significantly improved by the addition of PEG-TOCN. It was found that the reinforcing effect of PEG-TOCN in the DCM system was superior to that in the DMAc system, though the PEG-TOCNs were individually dispersed in both systems.[24,25] We anticipated from these results that the solvent used in preparation of composite films affected the miscibility of interfacial PEG layers in the CTA matrix. In this study, therefore, the influence of compatibility of PEG-grafted

Received: June 11, 2020
Accepted: August 26, 2020
Published: September 10, 2020

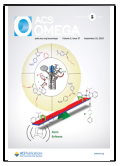

layers with the CTA matrix was investigated for the PEG-TOCN/CTA three-component system using different solvents in mixing, casting, and drying to prepare composite films.

In the present study, we investigated the relationship between interfacial miscibility of the grafted PEG/CTA matrix and the reinforcing effect of TOCNs on the CTA matrix. It has been reported that the dissolving solvent greatly affects the interfacial miscibility in polymer blends by the casting-drying method.[26−28] Hence, we prepared PEG-TOCN/CTA composite films from different solvents to control the interfacial miscibility between the grafted PEG chains on the TOCN surfaces and CTA matrix. The experimental parameters, such as the aspect ratio of TOCN, PEG grafting density on TOCN surfaces, drying rate of the solvent, and drying temperature in film preparation, were systematically controlled to selectively extract the effect of interfacial PEG layers on composite properties. The degrees of dispersion of PEG-grafted TOCN elements in the CTA matrix were assumed to be the same between the dried composite films prepared using different solvents based on transmission electron microscopy (TEM) images of PEG-TOCN/polymer composites reported in previous papers.[24,29] This study shows the significance of tuning the compatibility of surface layers on the nanofiller with the polymer matrix and will pave the way for controlling the material properties of CTA as transparent optical films by this method.

MATERIALS AND METHODS

Materials. A never-dried softwood bleached kraft pulp (SBKP) was supplied by Nippon Paper Industries Co., Ltd. (Tokyo, Japan). TEMPO was purchased from Sigma-Aldrich Japan. CTA (degree of polymerization, 270; degree of substitution, 2.87) was supplied by Daicel Corp. (Tokyo, Japan). Amine-terminated PEG (PEG-NH_2, SUNBRIGHT MEPA-20H, M_w = 2182) was purchased from NOF Corp. (Tokyo, Japan). All other reagents and solvents were purchased from FUJIFILM Wako Pure Chemical Corp. (Tokyo, Japan).

TEMPO-Mediated Oxidation. SBKP was oxidized with a TEMPO/sodium bromide/sodium hypochlorite system. The amount of sodium hypochlorite was adjusted to a 3.8 mmol/g pulp. The detailed conditions of the TEMPO-mediated oxidation have been reported elsewhere.[30] A small amount of C6-aldehyde groups and C2/C3 ketones formed as side reactions and present in the TEMPO-oxidized pulp[31] was selectively reduced with sodium borohydride, according to a previous report.[26] The amount of carboxy groups in the TEMPO-oxidized pulp was 1.19 mmol/g.

Preparation of PEG-TOCN/Organic Solvent Dispersions. The TEMPO-oxidized pulp was suspended in water at 0.1% w/w and subsequently disintegrated to prepare a TOCN/water dispersion. The detailed procedures were reported previously.[30,32] The TOCN/water dispersion was converted to a protonated TOCN (TOCN-COOH) gel, according to a previous study.[33] The TOCN-COOH gel was washed and suspended in *N*,*N*-dimethylacetamide (DMAc), dioxane (DOX), or dichloromethane (DCM) at 0.1% w/w. PEG-NH_2 was added to the TOCN-COOH/organic solvent suspension at a carboxy/amine molar ratio of 1:1 to introduce PEG chains on the TOCN surfaces. The PEG-TOCN/organic solvent dispersions were obtained by mechanical disintegration of the PEG-NH_2/TOCN-COOH gel/organic solvent suspension.[25]

Preparation of PEG-TOCN/CTA Composite Films. At room temperature, CTA was dissolved in DMAc, DOX, or DCM at 2% w/v. A PEG-TOCN/CTA composite film was prepared from the mixture of the PEG-TOCN/organic solvent dispersion and the CTA/organic solvent solution by casting-drying on a glass Petri dish. The evaporation rate of each solvent was controlled by covering the Petri dish with a polytetrafluoroethylene (PTFE) sheet with holes of 1 mm in diameter (Table S1 in the Supporting Information). The TOCN contents of the composite films were calculated according to eq 1 and adjusted to 2.5% w/w

$$\text{TOCN content in composite film (\%)} = \frac{\text{TOCN (g)}}{\text{TOCN (g)} + \text{PEG-NH}_2\text{(g)} + \text{CTA (g)}} \times 100 \quad (1)$$

Analyses. Fourier transform infrared (FT-IR) spectra of cast-dried PEG-TOCN films were measured. The grafting ratios of PEG chains on the surface carboxy groups were calculated from the intensity of the absorption peaks at 1600 and 1720 cm^{-1}. Wide-angle X-ray diffraction (WAXD) patterns of the composites were obtained using a diffractometer (RINT2000, Rigaku Corp., Tokyo, Japan) with Cu Kα radiation (λ = 1.5418 Å) at 40 kV and 40 mA. The optical and mechanical properties of the composites were measured, according to our previous studies.[23−25] Dynamic mechanical analysis in torsion was carried out using a stress-controlled rheometer (MCR 302, Anton Paar GmbH, Graz, Austria). The dynamic mechanical properties of the composites were measured from 30 to 220 °C with a heating rate of 5 °C min^{-1}, a frequency of 1 Hz, and a strain of 0.1%. The specimens for dynamic mechanical analysis were rectangular-shaped (40 × 5 mm). Three specimens were tested for each sample, and reported results are averages with standard deviations of these three values.

RESULTS AND DISCUSSION

Evaporation Rate of Solvents. It has been reported that the drying temperature and evaporation rate of the casting solvent affect the crystallinity-dependent mechanical and thermal properties of cast-dried polymer films.[34−38] Therefore, the drying temperature was fixed at 40 °C in the present study, and the evaporation rate was controlled at almost the same rate by covering the Petri dish with a PTFE sheet containing holes and changing the pressure during drying. The evaporation rate of the casting solvents was adjusted to match that of DMAc because DMAc has the highest boiling temperature and the slowest evaporation rate among the solvents used in the present study (Figure 1). The weight loss of the PEG-TOCN/CTA/solvent mixture became more than 95% between 270 and 300 min in all solvent systems. Accordingly, the effect of drying temperature and evaporation rate on the film properties could be minimized in the present study.

Crystallinity of CTA Matrix. Figure 2 shows WAXD patterns of the composite films. The crystallinities of the CTA matrix were calculated from the WAXD data with the Ruland−Vonk or amorphous contribution subtraction method (Table S2).[39,40] Peak positions corresponding to crystalline and amorphous CTA were determined, according to previous studies.[41,42]

As shown in Figure 2, all the composite films showed the typical WAXD pattern of CTA II.[43] The diffraction peak of the

https://dx.doi.org/10.1021/acsomega.0c02772
ACS Omega 2020, 5, 23755−23761

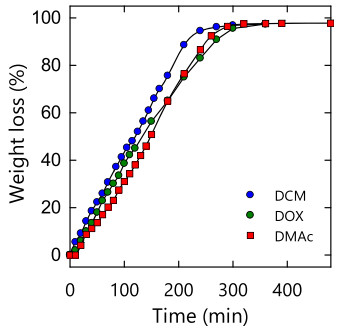

Figure 1. Weight loss of CTA solutions in each solvent during drying. DMAc: *N*,*N*-dimethylacetamide, DOX: dioxane, and DCM: dichloromethane.

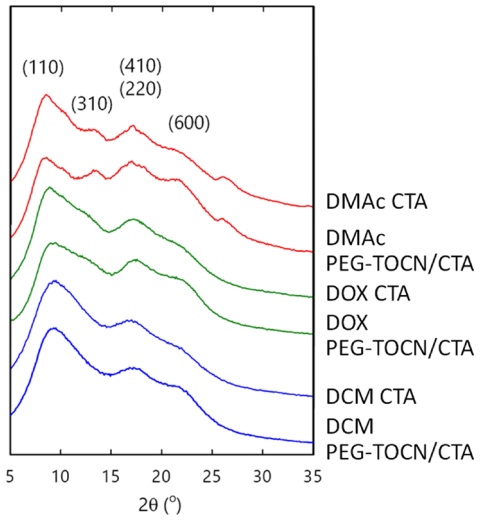

Figure 2. WAXD patterns of the composite films. DMAc: *N*,*N*-dimethylacetamide, DOX: dioxane, and DCM: dichloromethane. The TOCN content of the composite films was adjusted to 2.5% w/w.

composite films became sharper in the order of DMAc > DOX > DCM. The difference can be attributed to the solubility of CTA in each solvent. However, the films had similar crystallinities of ∼30%, which is typical for CTA cast films.[44,45] Although the crystallinity of the CTA matrix also showed a slight change after the addition of PEG-TOCN (Table S2), the difference in crystallinity between the pristine CTA and PEG-TOCN/CTA films was negligible. Hence, PEG-TOCN had no appreciable influence on the crystalline behavior of the CTA matrix, which is consistent with previous reports.[23,24]

Dynamic Mechanical Analysis of PEG-TOCN/CTA Composite Films. We conducted dynamic mechanical analysis of the composite films to investigate the miscibility at the interphase. Figure 3 shows representative tanδ curves for the composite films prepared from each solvent. The peak at ∼180 °C can be attributed to rearrangement of the CTA main chains in the amorphous region,[46] while the CTA degradation temperature occurs at ≥220 °C.[47] Thus, the peak in the tanδ curves reflects local molecular motions of cellulose backbones of the CTA matrix, regardless of casting conditions (Figure 3). The shoulder peak at 50−100 °C can be attributed to melting of PEG domains. In the DCM system, the shoulder peak at 50−150 °C was prominent compared to the other solvent systems. The detail will be discussed later.

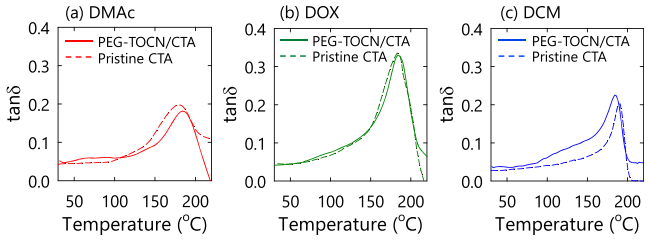

Figure 3. Representative tanδ curves of the composite films prepared from (a) *N*,*N*-dimethylacetamide (DMAc), (b) dioxane (DOX), and (c) dichloromethane (DCM). The TOCN content of the composite films was adjusted to 2.5% w/w.

The glass transition temperature (T_g) of the CTA matrix was calculated from the peak position in the tanδ curves, as shown in Figure 4. The T_g value of the CTA matrix slightly increased

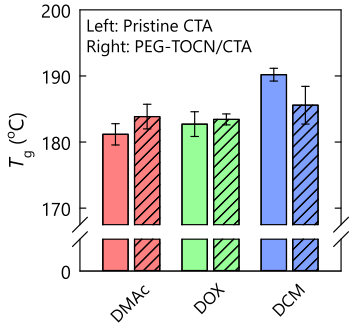

Figure 4. Glass transition temperatures of the composite films. The TOCN content of the composite films was adjusted to 2.5% w/w. DMAc: *N*,*N*-dimethylacetamide, DOX: dioxane, and DCM: dichloromethane.

from 181 to 183 °C or from 182 to 183 °C by the addition of PEG-TOCNs to the DMAc and DOX systems, respectively. In contrast, the T_g value for the PEG-NH_2/CTA composite film was always lower than that of the pristine CTA film prepared with any casting solvent (Figure S1). This indicates that free PEG chains plasticized the CTA matrix.

In the DMAc and DOX systems, the peak heights and widths in the tanδ curves were similar between the pristine CTA and PEG-TOCN/CTA composite films, and the peak position shifted to higher temperatures compared to the pristine CTA (Figure 3a,b). These results suggest that the grafted PEG chains and CTA matrix were not completely miscible at the interface and that the chain mobility of the CTA matrix in the vicinity of the PEG-TOCN/CTA interface was suppressed, resulting in the slight increase in T_g (Figure 5a).

In the DCM system, the peak positions of the PEG-TOCN/CTA composite films shifted to a lower temperature compared to the pristine CTA films. A new shoulder peak appeared at ∼150 °C (Figure 3c), and this shoulder peak can be attributed to the plasticizing effect of the grafted PEG chains. It is likely that the grafted PEG chains formed a miscible interphase with the CTA matrix (Figure 5b), resulting in the decrease in T_g. The plasticized CTA should have a different relaxation behavior compared with the bulk CTA matrix, which accounts for the peak broadening in the tanδ curves.

The differences in T_g can be also interpreted using the solubility parameters of the components. The properties of the components are shown in Table 1.[48−54] Using Hansen's three

https://dx.doi.org/10.1021/acsomega.0c02772
ACS Omega 2020, 5, 23755−23761

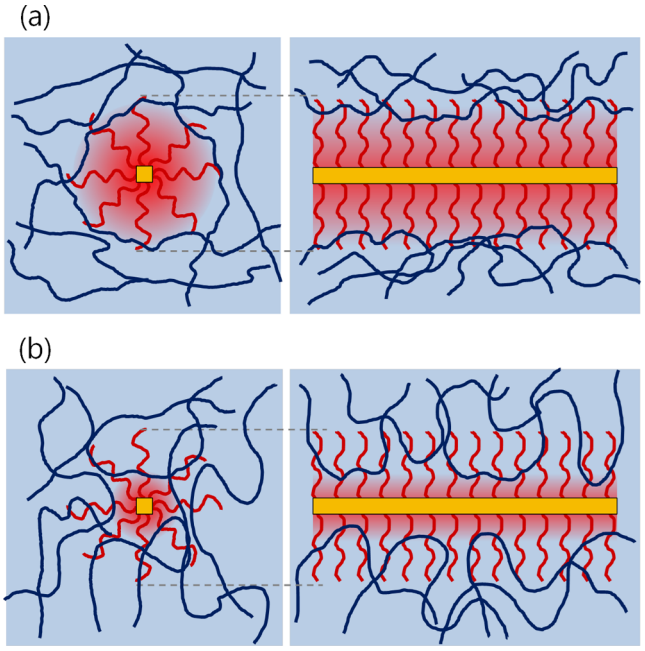

Figure 5. Schematic illustration of the interfacial layer structure of the composite films: (a) *N*,*N*-dimethylacetamide and dioxane systems and (b) dichloromethane system.

Table 1. Solubility Parameters of Organic Solvents and Polymers[48−54]

	DMAc	DOX	DCM	CTA	PEG
Hildebrand solubility parameter ($MPa^{-1/2}$)	22.5	20.5	19.8	18.8−19.4	20.2
Hansen solubility parameter ($MPa^{-1/2}$)					
δ_D	16.8	19	18.2	18.6	19.4
δ_P	11.5	1.8	6.3	12.7	1.6
δ_H	10.2	7.4	6.1	11	1.2
R_{CTA}	3.9	11.5	8.1		14.9
R_{PEG}	14.4	6.3	7.2	14.9	

components (δ_D, δ_P, and δ_H), a three-dimensional solubility diagram can be constructed in which a solvent or polymer is represented as a point.[47] The solubility is characterized by the distance between points of the solvent and polymer. Each polymer is defined as the center of the solubility sphere. The interaction radius R between the center of the sphere and the point of the solvent is given in eq 2

$$R = \{4(\delta_{Di} - \delta_{Dj})^2 + (\delta_{Pi} - \delta_{Pj})^2 + (\delta_{Hi} - \delta_{Hj})^2\}^{1/2} \quad (2)$$

where the subscripts i and j represent each component. In this study, R_{CTA} and R_{PEG} were calculated to estimate the solubility of CTA and PEG, respectively, for each organic solvent and polymer.

R_{CTA} and R_{PEG} in the DCM system showed similar small values of 8.1 and 7.2, respectively. This suggests that both CTA molecules and PEG chains behave as polymers dissolved in DCM and that these components can be intercalated to each other to form miscible and thick interphases (Figure 5b).[55] In contrast, DMAc or DOX has a lower R_{CTA} or R_{PEG} value but has a higher R_{CTA} or R_{PEG} value. Hence, DMAc or DOX may not behave as a good solvent for both CTA molecules and PEG chains but only for either CTA or PEG. The difference in solubility between the CTA molecules and PEG chains may have induced the partially intercalated interphase (Figure 5a).

Optical Properties of PEG-TOCN/CTA Composite Films. The light transmittances of the composite films are shown in Figure 6. The PEG-TOCN/CTA films had high optical transparency, showing a light transmittance of ∼90% at 400−800 nm, irrespective of the casting solvent. This suggests that the PEG-TOCNs were individually dispersed in the CTA matrix prepared by the solvent casting method used in this study. The transparency of the CTA films was not significantly affected by the CTA crystallinity.[44] However, we have to determine accurate degrees of TOCN dispersion in the composite films prepared using three different solvents in a future study.

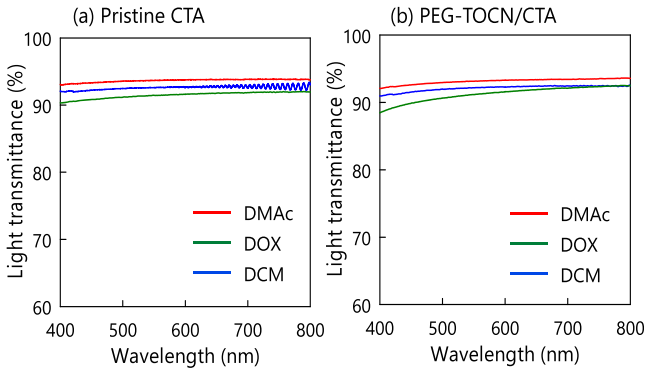

Figure 6. Light transmittance spectra of (a) pristine CTA and (b) PEG-TOCN/CTA composite films. The TOCN content of the composite films was adjusted to 2.5% w/w. DMAc: *N*,*N*-dimethylacetamide, DOX: dioxane, and DCM: dichloromethane.

Mechanical Properties of PEG-TOCN/CTA Composite Films. Representative stress−strain curves and corresponding mechanical properties of the composite films are shown in Figures 7 and 8, respectively. The toughness was calculated from the area under the stress−strain curves in the present study. Welch's unequal variances t test was performed to confirm the statistical significance of differences in mechanical properties of the pristine CTA and PEG-TOCN/CTA composite films (Table S3). The densities and water contents of the nanocomposite films were ∼1.2 g/cm^3 and ∼1.5%, respectively, in all the solvent systems (Table S3). Therefore,

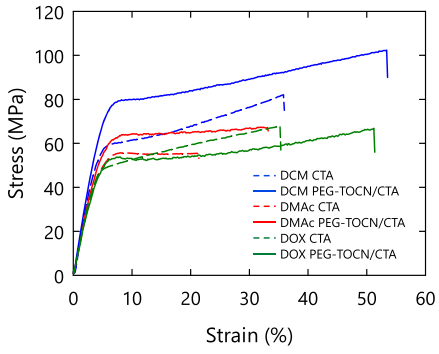

Figure 7. Representative stress−strain curves of the composite films. The TOCN content of the composite films was adjusted to 2.5% w/w. DMAc: *N*,*N*-dimethylacetamide, DOX: dioxane, and DCM: dichloromethane.

https://dx.doi.org/10.1021/acsomega.0c02772
ACS Omega 2020, 5, 23755−23761

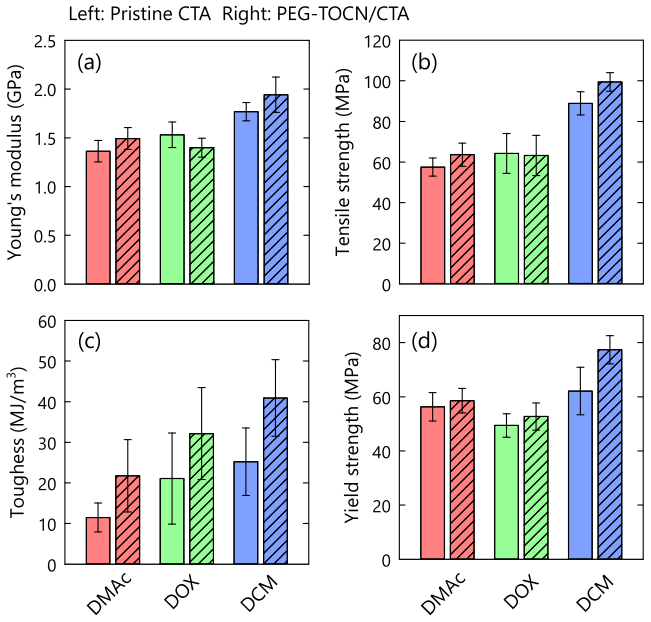

Figure 8. Mechanical properties of the composite films: (a) Young's modulus, (b) tensile strength, (c) toughness, and (d) yield strength. The TOCN content of the composite films was adjusted to 2.5% w/w. DMAc: *N*,*N*-dimethylacetamide, DOX: dioxane, and DCM: dichloromethane.

the mechanical properties of the composite films were not affected by the density or water content of the film.

As shown in Figure 7, the mechanical properties of both the pristine CTA and PEG-TOCN/CTA composite films showed different behaviors depending on the casting solvent. In the DMAc and DCM systems, Young's modulus and the tensile strength of the pristine CTA were improved by the addition of PEG-TOCN (p value <0.025; see Table S3). This result is similar to those reported previously.[23−25] The yielding strength of the CTA matrix was significantly improved in the DCM system by the addition of PEG-TOCN, while the other solvent systems showed no significant improvement (p value >0.025). This result suggests that the interaction between the TOCNs and CTA matrix was favorable[56] because of the formation of the miscible interphase and that an effective stress transfer occurred in the composite films prepared with the DCM system.

In the DOX system, an increase in Young's modulus or tensile strength was not observed. This indicates that the interaction between the PEG-TOCNs and CTA matrix was so weak that the stress transfer between the TOCNs and CTA matrix was inefficient, and thus, the reinforcing effect of the PEG-TOCNs was not exploited. This can be explained by the difference in the solubility parameter between the solvents, as discussed in the previous section; a soft PEG layer was partially intercalated with CTA matrices and hampered the stress transfer between TOCNs and CTA matrices. Specifically, a thick PEG-dominant layer was formed in the DOX system because PEG was seemed to be sufficiently swollen in DOX.

The toughness of CTA was improved by the addition of PEG-TOCNs in all the solvent systems. A ductile or tough pattern was not observed for the PEG-NH_2/CTA composites (see Figure S2 in the Supporting Information). Therefore, the PEG-TOCN components supported the plastic deformation of the CTA matrix and enhanced the energy dissipation during deformation. The composite films prepared from DCM showed a large plastic deformation after yielding and stress hardening. This behavior resulted in the highest toughness among the tested solvent systems. We investigated the effects of miscibility of surface PEG layers on TOCN in the CTA matrix on properties of the PEG-TOCN/CTA composite films using three different solvents. However, further studies are needed to determine accurate degrees of TOCN dispersion in the composite films prepared using three different solvents. The results obtained in this study have to be discussed also in terms of the degree of TOCN dispersion in the composite films and solubility of CTA in the three solvents at high CTA concentrations during the evaporation process.

CONCLUSIONS

We investigated the effects of miscibility of surface PEG layers on TOCN in the CTA matrix on properties of the PEG-TOCN/CTA composite films using three different solvents. The PEG-TOCN/CTA composite films showed high transparency irrespective of the miscibility. However, the mechanical properties of composite films differed between the different casting solvents, depending on the miscibility between the CTA molecules and PEG chains. These results indicate that the casting solvent affects not only the nature of the polymer matrix but also the interfacial structure between the nanofiller and polymer matrix. These results show that the material properties of nanocellulose/polymer composites can be improved by tuning the miscibility of surface-grafted layers on nanocellulose in the polymer matrix. Furthermore, the miscibility of the grafted layers in the polymer matrix is controllable by selecting the solvent used in mixing, casting, and drying processes in preparation of composite films.

ASSOCIATED CONTENT

Supporting Information

The Supporting Information is available free of charge at https://pubs.acs.org/doi/10.1021/acsomega.0c02772.

Drying conditions, crystallinities, glass transition temperatures, mechanical properties, and densities and water contents of PEG-TOCN/CTA composite films (PDF)

AUTHOR INFORMATION

Corresponding Author

Akira Isogai − *Department of Biomaterials Science, Graduate School of Agricultural and Life Sciences, The University of Tokyo, 113-8657 Tokyo, Japan;* orcid.org/0000-0001-8095-0441; Email: aisogai@mail.ecc.u-tokyo.ac.jp, +81 3 5841 5538

Authors

Hiroto Soeta − *Department of Biomaterials Science, Graduate School of Agricultural and Life Sciences, The University of Tokyo, 113-8657 Tokyo, Japan*

Shuji Fujisawa − *Department of Biomaterials Science, Graduate School of Agricultural and Life Sciences, The University of Tokyo, 113-8657 Tokyo, Japan;* orcid.org/0000-0002-5221-6781

Tsuguyuki Saito − *Department of Biomaterials Science, Graduate School of Agricultural and Life Sciences, The University of Tokyo, 113-8657 Tokyo, Japan;* orcid.org/0000-0003-1073-6663

Complete contact information is available at: https://pubs.acs.org/10.1021/acsomega.0c02772

https://dx.doi.org/10.1021/acsomega.0c02772
ACS Omega 2020, 5, 23755−23761

Notes

The authors declare no competing financial interest.

■ ACKNOWLEDGMENTS

This research was supported by Grants-in-Aid for Scientific Research (grant number 16J02980) from the Japan Society for the Promotion of Science (JSPS) and in part by the JST-Mirai Program (grant number JPMJMI17ED) and JSPS Grant-in-Aid for Young Scientists (grant number 17K15298). The authors thank the Edanz Group for editing a draft of this manuscript.

■ REFERENCES

(1) Fu, S.; Sun, Z.; Huang, P.; Li, Y.; Hu, N. Some Basic Aspects of Polymer Nanocomposites: A Critical Review. *Nano Mater. Sci.* **2019**, *1*, 2−30.
(2) Kotal, M.; Bhowmick, A. K. Polymer Nanocomposites from Modified Clays: Recent Advances and Challenges. *Prog. Polym. Sci.* **2015**, *51*, 127−187.
(3) Miao, C.; Hamad, W. Y. Critical Insights into the Reinforcement Potential of Cellulose Nanocrystals in Polymer Nanocomposites. *Curr. Opin. Solid State Mater. Sci.* **2019**, *23*, 100761.
(4) Li, Y.; Huang, X.; Zeng, L.; Li, R.; Tian, H.; Fu, X.; Wang, Y.; Zhong, W. H. A Review of the Electrical and Mechanical Properties of Carbon Nanofiller-Reinforced Polymer Composites. *J. Mater. Sci.* **2019**, *54*, 1036−1076.
(5) Kumar, A.; Sharma, K.; Dixit, A. R. A Review of the Mechanical and Thermal Properties of Graphene and Its Hybrid Polymer Nanocomposites for Structural Applications. *J. Mater. Sci.* **2019**, *54*, 5992−6026.
(6) Rafiee, R.; Shahzadi, R. Mechanical Properties of Nanoclay and Nanoclay Reinforced Polymers: A Review. *Polym. Compos.* **2019**, *40*, 431−445.
(7) Missoum, K.; Belgacem, M.; Bras, J. Nanofibrillated Cellulose Surface Modification: A Review. *Materials* **2013**, *6*, 1745−1766.
(8) Kango, S.; Kalia, S.; Celli, A.; Njuguna, J.; Habibi, Y.; Kumar, R. Surface Modification of Inorganic Nanoparticles for Development of Organic-Inorganic Nanocomposites - A Review. *Prog. Polym. Sci.* **2013**, *38*, 1232−1261.
(9) Kim, S. W.; Kim, T.; Kim, Y. S.; Choi, H. S.; Lim, H. J.; Yang, S. J.; Park, C. R. Surface Modifications for the Effective Dispersion of Carbon Nanotubes in Solvents and Polymers. *Carbon* **2012**, *50*, 3−33.
(10) Kalia, S.; Boufi, S.; Celli, A.; Kango, S. Nanofibrillated Cellulose: Surface Modification and Potential Applications. *Colloid Polym. Sci.* **2014**, *292*, 5−31.
(11) Kaldéus, T.; Träger, A.; Berglund, L. A.; Malmström, E.; Lo Re, G. Molecular Engineering of the Cellulose-Poly(Caprolactone) Bio-Nanocomposite Interface by Reactive Amphiphilic Copolymer Nanoparticles. *ACS Nano* **2019**, *13*, 6409−6420.
(12) Ma, P. C.; Siddiqui, N. A.; Marom, G.; Kim, J. K. Dispersion and Functionalization of Carbon Nanotubes for Polymer-Based Nanocomposites: A Review. *Compos. Part A Appl. Sci. Manuf.* **2010**, *41*, 1345−1367.
(13) Habibi, Y. Key Advances in the Chemical Modification of Nanocelluloses. *Chem. Soc. Rev.* **2014**, *43*, 1519−1542.
(14) Xie, L.; Xu, F.; Qiu, F.; Lu, H.; Yang, Y. Single-Walled Carbon Nanotubes Functionalized with High Bonding Density of Polymer Layers and Enhanced Mechanical Properties of Composites. *Macromolecules* **2007**, *40*, 3296−3305.
(15) Spitalsky, Z.; Tasis, D.; Papagelis, K.; Galiotis, C. Carbon Nanotube-Polymer Composites: Chemistry, Processing, Mechanical and Electrical Properties. *Prog. Polym. Sci.* **2010**, *35*, 357−401.
(16) Chadwick, R. C.; Khan, U.; Coleman, J. N.; Adronov, A. Polymer Grafting to Single-Walled Carbon Nanotubes: Effect of Chain Length on Solubility, Graft Density and Mechanical Properties of Macroscopic Structures. *Small* **2013**, *9*, 552−560.
(17) Chevigny, C.; Jouault, N.; Dalmas, F.; Boué, F.; Jestin, J. Tuning the Mechanical Properties in Model Nanocomposites: Influence of the Polymer-Filler Interfacial Interactions. *J. Polym. Sci., Part B: Polym. Phys.* **2011**, *49*, 781−791.
(18) Chevigny, C.; Dalmas, F.; Di Cola, E.; Gigmes, D.; Bertin, D.; Boué, F.; Jestin, J. Polymer-Grafted-Nanoparticles Nanocomposites: Dispersion, Grafted Chain Conformation, and Rheological Behavior. *Macromolecules* **2011**, *44*, 122−133.
(19) Sharma, S. C.; Sheshadri, T. S.; Krishna, M.; Murthy, H. N. N.; Jose, J. Influence of Solvents on the MWCNT/Adhesive Grade Epoxy Nanocomposites Preparation. *J. Reinf. Plast. Compos.* **2009**, *28*, 2805−2812.
(20) Rizvi, R.; Kim, J. K.; Naguib, H. The Effect of Processing and Composition on the Properties of Polylactide-Multiwall Carbon Nanotube Composites Prepared by Solvent Casting. *Smart Mater. Struct.* **2010**, *19*, 094003.
(21) Jouault, N.; Zhao, D.; Kumar, S. K. Role of Casting Solvent on Nanoparticle Dispersion in Polymer Nanocomposites. *Macromolecules* **2014**, *47*, 5246−5255.
(22) Lau, K.; Lu, M.; Cheung, H.; Sheng, F.; Li, H. Thermal and Mechanical Properties of Single-Walled Carbon Nanotube Bundle-Reinforced Epoxy Nanocomposites: The Role of Solvent for Nanotube Dispersion. *Compos. Sci. Technol.* **2005**, *65*, 719−725.
(23) Soeta, H.; Fujisawa, S.; Saito, T.; Isogai, A. Interfacial Layer Thickness Design for Exploiting the Reinforcement Potential of Nanocellulose in Cellulose Triacetate Matrix. *Compos. Sci. Technol.* **2017**, 100−106.
(24) Soeta, H.; Lo Re, G.; Masuda, A.; Fujisawa, S.; Saito, T.; Berglund, L. A.; Isogai, A. Tailoring Nanocellulose-Cellulose Triacetate Interfaces by Varying the Surface Grafting Density of Poly(Ethylene Glycol). *ACS Omega* **2018**, *3*, 11883−11889.
(25) Fujisawa, S.; Saito, T.; Kimura, S.; Iwata, T.; Isogai, A. Surface Engineering of Ultrafine Cellulose Nanofibrils toward Polymer Nanocomposite Materials. *Biomacromolecules* **2013**, *14*, 1541−1546.
(26) Wu, W. B.; Chiu, W. Y.; Liau, W. B. Casting Solvent Effect on Crystallization Behavior of Poly (Vinyl Acetate)/Poly (Ethylene Oxide) Blends: DSC Study. *J. Appl. Polym. Sci.* **1996**, *64*, 411−421.
(27) Cui, L.; Ding, Y.; Li, X.; Wang, Z.; Han, Y. Solvent and Polymer Concentration Effects on the Surface Morphology Evolution of Immiscible Polystyrene/Poly (Methyl Methacrylate) Blends. *Thin Solid Films* **2006**, *515*, 2038−2048.
(28) Tang, M.; Liau, W.-R. Solvent Effect on the Miscibility of Poly (4-Hydroxystyrene)/Poly (Ethylene Oxide) Blends. *Eur. Polym.. J.* **2000**, *36*, 2597−2603.
(29) Fujisawa, S.; Saito, T.; Kimura, S.; Iwata, T.; Isogai, A. Comparison of Mechanical Reinforcement Effects of Surface-Modified Cellulose Nanofibrils and Carbon Nanotubes in PLLA Composites. *Compos. Sci. Technol.* **2014**, *90*, 96−101.
(30) Saito, T.; Nishiyama, Y.; Putaux, J. L.; Vignon, M.; Isogai, A. Homogeneous Suspensions of Individualized Microfibrils from TEMPO-Catalyzed Oxidation of Native Cellulose. *Biomacromolecules* **2006**, *7*, 1687−1691.
(31) Saito, T.; Isogai, A. Introduction of Aldehyde Groups on Surfaces of Native Cellulose Fibers by TEMPO-Mediated Oxidation. *Colloids Surfaces A* **2006**, *289*, 219−225.
(32) Saito, T.; Kimura, S.; Nishiyama, Y.; Isogai, A. Cellulose Nanofibers Prepared by TEMPO-Mediated Oxidation of Native Cellulose. *Biomacromolecules* **2007**, *8*, 2485−2491.
(33) Okita, Y.; Fujisawa, S.; Saito, T.; Isogai, A. TEMPO-Oxidized Cellulose Nanofibrils Dispersed in Organic Solvents. *Biomacromolecules* **2011**, *12*, 518−522.
(34) Strawhecker, K. E.; Kumar, S. K.; Douglas, J. F.; Karim, A. The Critical Role of Solvent Evaporation on the Roughness of Spin-Cast Polymer Films. *Macromolecules* **2001**, *34*, 4669−4672.
(35) Sakurai, S.; Furukawa, C.; Okutsu, A.; Miyoshi, A.; Nomura, S. Control of Mesh Pattern of Surface Corrugation via Rate of Solvent Evaporation in Solution Casting of Polymer Film in the Presence of Convection. *Polymer* **2002**, *43*, 3359−3364.
(36) Yang, X.; van Duren, J. K. J.; Rispens, M. T.; Hummelen, J. C.; Janssen, R. A. J.; Michels, M. A. J.; Loos, J. Crystalline Organization of

https://dx.doi.org/10.1021/acsomega.0c02772
ACS Omega 2020, 5, 23755−23761

a Methanofullerene as Used for Plastic Solar-Cell Applications. *Adv. Mater.* **2004**, *16*, 802−806.
(37) Chinaglia, D. L.; Gregorio, R., Jr.; Stefanello, J. C.; Altafim, R. A. P.; Wirges, W.; Wang, F.; Gerhard, R. Influence of the Solvent Evaporation Rate on the Crystalline Phases of Solution-Cast Poly(Vinylidene Fluoride) Films. *J. Appl. Polym. Sci.* **2010**, *116*, 785−791.
(38) Katsumata, R.; Ata, S.; Kuboyama, K.; Ougizawa, T. Evaporation Rate Effect on Starting Point of Shrinkage Stress Development during Drying Process in Solvent Cast Polymer Film. *J. Appl. Polym. Sci.* **2013**, *128*, 60−65.
(39) de Freitas, R. R. M.; Senna, A. M.; Botaro, V. R. Influence of Degree of Substitution on Thermal Dynamic Mechanical and Physicochemical Properties of Cellulose Acetate. *Ind. Crops Prod.* **2017**, *109*, 452−458.
(40) Karimi, K.; Taherzadeh, M. J. A Critical Review of Analytical Methods in Pretreatment of Lignocelluloses: Composition, Imaging, and Crystallinity. *Bioresour. Technol.* **2016**, *200*, 1008−1018.
(41) Hindeleh, A. M.; Johnson, D. J. Correlation Crystallinity and Physical Properties of Heat-Treated Cellulose Triacetate Fibres. *Polymer* **1970**, *11*, 666−680.
(42) Hindeleh, A. M.; Johnson, D. J. Peak Resolution and X-Ray Crystallinity Determination in Heat-Treated Cellulose Triacetate. *Polymer* **1972**, *13*, 27−32.
(43) Zugenmaier, P. Characterization and Physical Properties of Cellulose Acetates. *Macromol. Symp.* **2004**, *208*, 81−166.
(44) Songsurang, K.; Miyagawa, A.; Manaf, M. E. A.; Phulkerd, P.; Nobukawa, S.; Yamaguchi, M. Optical Anisotropy in Solution-Cast Film of Cellulose Triacetate. *Cellulose* **2013**, *20*, 83−96.
(45) Sata, H.; Murayama, M.; Shimamoto, S. Properties and Applications of Cellulose Triacetate Film. *Macromol. Symp.* **2004**, *208*, 323−334.
(46) Manabe, S.; Iwata, M.; Kamide, K. Dynamic Mechanical Absorptions Observed for Regenerated Cellulose Solids in the Temperature Range from 280 to 600 K. *Polym. J.* **1986**, *18*, 1−14.
(47) Alves Cerqueira, D.; Rodrigues Filho, G.; De Assuncão, R. M. N.; Da Silva Meireles, C.; Cardoso Toledo, L.; Zeni, M.; Mello, K.; Duarte, J. Characterization of Cellulose Triacetate Membranes, Produced from Sugarcane Bagasse, Using PEG 600 as Additive. *Polym. Bull.* **2008**, *60*, 397−404.
(48) Smallwood, I. M. Handbook of Organic Solvent Properties. *Int. J. Adhes. Adhes.* **1997**, *17*, 177.
(49) Hansen, C. M. *Hansen Solubility Parameters: A User's Handbook*, Second Ed.; CRC Press, 2007.
(50) Adamska, K.; Voelkel, A. Hansen Solubility Parameters for Polyethylene Glycols by Inverse Gas Chromatography. *J. Chromatogr. A* **2006**, *1132*, 260−267.
(51) Cobo, F. N.; Faria-Tisher, P. C. S.; Duarte, J. L.; Carvalho, G. M. Preparation and Characterization of Microporous Cellulose Acetate Films Using Breath Figure Method by Spin Coating Technique. *Cellulose* **2017**, *24*, 4981−4995.
(52) Lu, H. T.; Kanehashi, S.; Scholes, C. A.; Kentish, S. E. The Impact of Ethylene Glycol and Hydrogen Sulphide on the Performance of Cellulose Triacetate Membranes in Natural Gas Sweetening. *J. Memb. Sci.* **2017**, *539*, 432−440.
(53) Nguyen, T. P. N.; Yun, E. T.; Kim, I. C.; Kwon, Y. N. Preparation of Cellulose Triacetate/Cellulose Acetate (CTA/CA)-Based Membranes for Forward Osmosis. *J. Memb. Sci.* **2013**, *433*, 49−59.
(54) Bock, N.; Dargaville, T. R.; Woodruff, M. A. Controlling Microencapsulation and Release of Micronized Proteins Using Poly(Ethylene Glycol) and Electrospraying. *Eur. J. Pharm. Biopharm.* **2014**, *87*, 366−377.
(55) Bui, V. T.; Baril, D.; Vu, T. L. Solvent Effect on the Miscibility of Polymer Blends. *Makromol. Chem.* **1988**, *16*, 267−279.
(56) Zare, Y. Estimation of Material and Interfacial/Interphase Properties in Clay/Polymer Nanocomposites by Yield Strength Data. *Appl. Clay Sci.* **2015**, *115*, 61−66.

https://dx.doi.org/10.1021/acsomega.0c02772
ACS Omega 2020, 5, 23755−23761